Journal of Cosmology and
Astroparticle Physics

Proca stars with dark photons from spontaneous symmetry breaking of the scalar field dark matter

Journal of Cosmology and Astroparticle Physics
An IOP and SISSA journal

Proca stars with dark photons from spontaneous symmetry breaking of the scalar field dark matter

Leonardo San.-Hernandez[a] **and Tonatiuh Matos**[b]

[a]Departamento de Física, Universidad Autónoma Metropolitana Iztapalapa, Av. San Rafael Atlixco 186, Ciudad de México 09340, México
[b]Departamento de Física, Centro de Investigación y de Estudios Avanzados del IPN, A.P. 14-740, Ciudad de México 07000, México

E-mail: leonardo.sanchez@cinvestav.mx, tonatiuh.matos@cinvestav.mx

Received May 11, 2023
Revised September 2, 2023
Accepted November 28, 2023
Published January 11, 2024

Abstract. Recently, the Scalar Field Dark Matter (SFDM) model (also known as Fuzzy, Wave, Bose-Einstein, Ultra-light Dark Matter) has gained a lot of attention because it has provided simpler and more natural explanations for various phenomena observed in galaxies, as a natural explanation for the center of galaxies, the number of satellite galaxies around their host and, more recently, a natural explanation for anomalous trajectories of satellite galaxies called Vast Polar Orbits (VPO) observed in various galaxies. In the present work we study the assumption that the SFDM is a type of charged dark boson whose gauge charge is associated with the Dark Photon (DP). Inspired by these results, we study the formation of compact bosonic objects, such as Boson Stars (BS) and focus on the possibility that, due to spontaneous U(1) SFDM symmetry breaking, the DP may acquire mass and form compact objects like Proca Stars (PS). If this is true, we can expect measurable effects on the electromagnetic field of the Standard Model (SM) of particles due to their interaction with the DP on the formation of compact objects.

Keywords: dark matter theory, gravity, quantum field theory on curved space, star formation

ArXiv ePrint: 2305.05674

https://doi.org/10.1088/1475-7516/2024/01/018

JCAP01(2024)018

Contents

JCAP01(2024)018

1 Introduction

Dark Matter (DM) is one of the most fascinating open problems in physics. The Cold Dark Matter (CDM) model has been one of the most widely used to attempt to explain dark matter; however, this model presents a number of difficulties in making predictions on a galactic scale. Because of this, alternative models that are consistent with the observations have been proposed; the Scalar Field Dark Matter is one of these models.

The idea of SFDM model was proposed in 1994 by Ji S.U. & Sin S.J. [1], and Lee & Koh in 1996 [2], and later independently by Siddharta & Matos in 1998 [3]. It was during these years that continued research on scalar field dark matter began. Historical and analytical reviews on the evolution of this model can be found in [4–9]. The SFDM model has been rediscovered over the years and has been given different names: Fuzzy Dark Matter (2000) [10], Quintessential Dark Matter (2001) [11], Wave Dark Matter (2010) [12] and Ultralight Dark Matter (ULDM), which classifies scalar field dark matter based on its condensation structure [13].

In general, the SFDM model proposes that dark matter consists of spin-zero ultralight massive bosons associated with a scalar field Φ that only interacts gravitationally with baryonic matter. So, the SFDM must satisfy an equation of the type Klein-Gordon, and the dynamics of the universe can be found by combining the Lagrangian of this model with gravity in the Einstein equations.

One of the most fascinating characteristics of SFDM is its quantum nature, recently studied in [14]. Due to this property, the SFDM model is capable of explaining phenomena such as the vast polar orbits of satellite galaxies around their host, the so-called VPO [15], observed in systems such as the Milky Way, Andromeda, and Cen A. The VPOs are explained using excited states of the scalar field. At galactic regimes, non-relativistic behavior and weak fields can be assumed for the system. In this approximation, the Einstein-Klein-Gordon system that describes the SFDM is reduced to a Schrödinger-Poisson system, so that the

system can be in the ground state or excited states (or both) in analogy to an atom. The excited states produce an 8-shaped structure, which may explain the alignment of the satellite galaxies on polar trajectories around the host galaxies. This is a remarkable result as no other DM model can adequately explain these phenomena in such a natural way.

On the other hand, exotic compact objects, also known as exotic stars or bosonic stars, have also gained great relevance in recent years due to their ability to mimic significant astrophysical phenomena such as Black Hole Shadows (BHS) [16–18] and Gravitational Wave Events (GW) [19]. This becomes even more important with the discovery of the Higgs boson in 2012, since this was a reaffirmation of the existence of bosons in nature (although the Higgs boson is too unstable to be a candidate to form boson stars [20]). In general, the term Bosonic Star (BSS) refers to hypothetical astrophysical compact objects composed fundamentally of ultralight bosons [16]. If the star is composed of bosons with spin $s = 0$, it is known as Boson Star (described by scalar fields) [21], and if it is composed of bosons with spin $s = 1$, it is known as Proca Star (described by vector fields) [22]. Both PS and BS have been studied in the context of DM. In [23] BS were studied at galactic scales, and it was found that for scalar bosons of mass $m \sim 10^{-23}\,\text{eV}$ it is possible to obtain stars of mass $M \sim 10^{12}\,M_{\odot}$ and radius $R \sim 10^{13}\,\text{km}$. These results are compatible with the SFDM model for the formation of galactic nuclei presented in [24]. On the other hand, PS have been used to make simulations that mimic black hole observables. This is possible because, unlike the BS, the PS possess a robust formational dynamics process [25]. In [19], for example, the gravitational wave event GW190521 was simulated using the collision of two rotating PS, and when the results were compared to the observational data, it was found that this model fits the event a little better than the one proposed by the LIGO-Virgo collaboration [25]. While in [16] it was shown that PS are capable of producing shadows similar to those of a Schwarzschild black hole if the observation is made from a polar angle similar to the position of the earth with respect to M87. Then, the capability of PS to mimic dark objects such as black holes motivates the possibility of being studied by DM models. Despite these results, it is important to mention that the dynamical robustness of the Proca model is compromised in the presence of self-interactions; this is due to the emergence of hyperbolic issues and instabilities, as has been pointed out in [26–30]. Solutions to these problems have been proposed in [31, 32]; these proposals involve partial UV completions for the Proca model, so that the dynamic issues arise only in the effective theory but not in the complete theory. Therefore, these difficulties must be taken into account in the study of Proca-like models such as the one proposed in this work.

Inspired by all these results, in this work we study the possibility of obtaining BS and PS by imposing particular constraints on the SFDM model proposed in [33]. In particular, we consider the case where the DP associated with the U(1) gauge symmetry of the model can acquire mass due to the spontaneous symmetry breaking of the system and then form compact objects such as Proca stars. By doing this, we find that the formation of Proca stars has effects on the electromagnetic field of the SM due to the mixing terms between the DP and the SM photon. This is very important because it means that the formation of these compact objects causes changes in the electromagnetic field of the SM that, in principle, we could measure.

In section 2 we present the general SFDM model that we use and the derivation of some particular cases such as BS and CBS. In section 3, we present the physical mechanism for the spontaneous symmetry breaking considering that the scalar field is inside a thermal bath, and therefore there is a cut-off term for the temperature that can cause the spontaneous

JCAP01(2024)018

symmetry breaking through which the DP acquires mass. In section 4, we focus on the Proca stars formed by dark photons that acquire mass via the Higgs mechanism induced by the SFDM, and we study the effects of this process on the maximal mass of the Proca stars. In section 5, we study the case of Proca stars when the coupling between the DP and SM photon is manifest. Finally, in sections 6 and 7, we present the numerical results and the effects of this process on the electromagnetic field of the SM.

2 U(1)-SFDM model

Thus, we start with the Lagrangian proposed in [33]

$$\mathcal{L}=-\left(\nabla_\mu\Phi+iqB_\mu\Phi\right)\left(\nabla^\mu\Phi^*-iqB^\mu\Phi^*\right)-V\left(\Phi\right)-\frac{1}{4}F_{\mu\nu}F^{\mu\nu}-\frac{1}{4}B_{\mu\nu}B^{\mu\nu}-\frac{\delta^2}{2}F_{\mu\nu}B^{\mu\nu}, \quad (2.1)$$

where Φ is the complex scalar dark matter field; B_μ is the DP field associated to the U(1) local symmetry of the SFDM, with fundamental charge q and Faraday tensor defined as $B_{\mu\nu}=\nabla_\mu B_\nu-\nabla_\nu B_\mu$; A_μ is the 4-potential of the electromagnetic field of the standard model, with Faraday tensor defined as $F_{\mu\nu}=\nabla_\mu A_\nu-\nabla_\nu A_\mu$; $V\left(\Phi\right)$ is the potential associated to Φ, and δ^2 is the kinetic mixing parameter which couples the fields A_μ and B_μ. We use the standard general relativity signature $(-,+,+,+)$ in this work and the natural units $\hbar=c=k_\beta=\epsilon_0=1$. In general, to obtain separable solutions in the study of compact objects, we consider the fields A_μ and B_μ to be complex (each can be described in terms of two real fields), so the real part of A_μ corresponds to the physical electromagnetic field of the SM. Thus we rewrite the Lagrangian (2.1) as follows

$$\mathcal{L}=-\left(\nabla_\mu\Phi+iqB_\mu\Phi\right)\left(\nabla^\mu\Phi^*-iqB^{*\mu}\Phi^*\right)-V(\Phi)-\frac{1}{4}F_{\mu\nu}F^{*\mu\nu}-\frac{1}{4}B_{\mu\nu}B^{*\mu\nu}-\frac{\delta^2}{2}R_e\left\{F_{\mu\nu}B^{\mu\nu}\right\}. \quad (2.2)$$

It is important to notice that making A_μ and B_μ complex results in the addition of one extra vector field for each one, so the U(1) local symmetry for the SFDM model (2.1) may no longer be present. However, this local symmetry is recovered by constraining A_μ and B_μ to be real vector fields directly in the Lagrangian (2.2), as is the case for BS, CBS, and SSB. In the case of PS, which is studied in sections 4 and 5, the complex field approximation introduces a global symmetry U(1) for the system, which is relevant for the study of PS dynamics. The reason for proceeding in this way is solely to obtain a time-independent system of differential equations when solving the Einstein-Proca system. Therefore, this procedure is valid as long as the correct constraints are applied to preserve the appropriate symmetries in each particular case studied in this work. We couple this Lagrangian minimally with gravity in an action S of the form

$$S=\int d^4x\sqrt{-g}\left[\frac{1}{16\pi G}R+\mathcal{L}\right], \quad (2.3)$$

where R is the Ricci scalar, g is the determinant of the metric $g_{\mu\nu}$ and G is the Newton's constant. By varying this action with respect to the metric, we derive Einstein's field equations $G_{\alpha\mu}=8\pi GT_{\alpha\mu}$, where the energy-momentum tensor reads

$$\begin{aligned}T_{\alpha\mu}=&\,g_{\alpha\mu}\mathcal{L}+\left(\nabla_\mu\Phi+iqB_\mu\Phi\right)\left(\nabla_\alpha\Phi^*-iqB^*_\alpha\Phi^*\right)+\left(\nabla_\alpha\Phi+iqB_\alpha\Phi\right)\left(\nabla_\mu\Phi^*-iqB^*_\mu\Phi^*\right)\\&-F_{\nu(\alpha}F^{*\nu}_{\mu)}-B_{\nu(\alpha}B^{*\nu}_{\mu)}-2\delta^2\,\mathrm{Re}\left[F_{\nu(\alpha}B^{\ \nu}_{\mu)}\right].\end{aligned} \quad (2.4)$$

JCAP01(2024)018

The variation of the action S with respect to Φ, A_μ, and B_μ, gives the following equations of motion, respectively

$$\left(\nabla^\mu + iqB^{*\mu}\right)\left(\nabla_\mu\Phi + iqB_\mu\Phi\right) - \frac{dV\left(\Phi\Phi^*\right)}{d|\Phi|^2}\Phi = 0, \tag{2.5}$$

$$\nabla_\mu F^{\mu\nu} + \delta^2\nabla_\mu B^{*\mu\nu} = 0, \tag{2.6}$$

$$\nabla_\mu B^{\mu\nu} + \delta^2\nabla_\mu F^{*\mu\nu} = -2iq\Phi^*\left(\nabla^\nu\Phi + iqB^\nu\Phi\right). \tag{2.7}$$

As we can see, the equation (2.5) corresponding to the variation of Φ is a Klein-Gordon-type equation with a modified gauge covariant derivative that makes the complex nature of B_μ manifest. Additionally, the equation (2.6) corresponding to the variation of A_μ describes the coupled electrodynamics of the SM photon with the DP. Finally, the equation (2.7) from the variation of B_μ contains the electrodynamics of the DP coupled with the SM photon, along with the term that makes the coupling between B_μ and Φ manifest. We can impose particular constraints on this system to find different cases of compact objects formed by SFDM bosons. For example, by imposing $A_\mu = B_\mu = 0$ (which corresponds to regimes where electromagnetic fields are negligible) in the Lagrangian (2.2) we obtain the action $S_{\rm BS}$ associated to scalar boson stars of the form

$$S_{\rm BS} = \int d^4x\sqrt{-g}\left[\frac{R}{16\pi G} - \nabla_\mu\Phi\nabla^\mu\Phi^* - V\left(\Phi\right)\right]. \tag{2.8}$$

In the same way, if we now consider $A_\mu = 0$ and B_μ real in (2.2), we find the action $S_{\rm CBS}$ that describes charged boson stars (CBS)

$$S_{\rm CBS} = \int d^4x\sqrt{-g}\left[\frac{R}{16\pi G} + \mathcal{L}_{\rm CBS}\right], \tag{2.9}$$

where

$$\mathcal{L}_{\rm CBS} = -\left(\nabla_\mu\Phi + iqB_\mu\Phi\right)\left(\nabla^\mu\Phi^* - iqB^\mu\Phi^*\right) - V\left(\Phi\right) - \frac{1}{4}B_{\mu\nu}B^{\mu\nu}. \tag{2.10}$$

In both cases, BS and CBS are formed by SFDM ultralight bosons, and the charge q of the scalar field in CBS is associated with the dark photon. Although we have seen so far that it is possible to recover the associated Lagrangians for BS and CBS from the Lagrangian (2.2) by setting A_μ and B_μ to be real and zero, as the case may be, it is important to note that this is not a solution to the equations of motion (2.5)–(2.7) of the complete model. Therefore, if we wanted to study solutions for the complete model (2.2), it would be necessary to directly solve (2.5)–(2.7). In general, the SFDM model assumes ultralight boson masses between 1–10^{-24} eV [13], whereas models of bosonic stars in the literature assume masses for bosonic particles of approximately 10^{-10}–10^{-20} eV to obtain stars of astrophysical interest with maximal masses of approximately 1–$10^{10}\,M_\odot$ [25]. Then, we can consider compatible mass ranges to use the boson star literature results to study these compact objects in the context of SFDM presented here. See for example [16] for general solutions in BS and [34] for solutions in CBS.

The particular case that concerns us in this work is to consider a Higgs-type potential for the scalar field of dark matter so that the dark photon field B_μ can acquire mass through an spontaneous symmetry braking (SSB) of the system and then form compact objects like Proca Stars (PS). In the next section, we propose a thermal bath for Φ as a physical mechanism for the SSB. Thus, there is a range of temperatures and a cutoff temperature for SSB to occur.

JCAP01(2024)018

3 Spontaneous symmetry breaking

In order to consider a Higgs-type potential for the SFDM model (2.2), we propose that the complex scalar field of dark matter is in a thermal bath at temperature T, which is characterized by the potential of the form [35, 36]

$$V = -m_\Phi^2 \Phi\Phi^* + \frac{\lambda}{2}(\Phi\Phi^*)^2 + \frac{\lambda}{4}\Phi\Phi^* T^2 + \frac{\pi^2}{90}T^4, \tag{3.1}$$

where m_Φ is the mass parameter of the scalar field Φ, and λ is the self-interaction parameter. In this work we just consider the case $\lambda > 0$ (repulsive interactions). It is convenient to redefine the zero potential value of this potential and factorize V as follows

$$V = \frac{\lambda}{2}\left(\Phi\Phi^* - \frac{m^2}{\lambda}\right)^2, \tag{3.2}$$

where we define the effective mass parameter m of the scalar field as

$$m^2 \equiv \pm m_\Phi^2\left(1 - \frac{\lambda}{4m_\Phi^2}T^2\right). \tag{3.3}$$

The plus and minus signs in this definition depend on the sign of the expression between parentheses. To illustrate this, we define the spontaneous symmetry breaking parameter as $\eta \equiv (1 - \lambda T^2/4m_\Phi^2)$. If $\eta > 0$, then m^2 is given by the plus sign in (3.3). In this case the potential (3.2) describes a Higgs-type potential (Mexican hat shape), and therefore we can expect a SSB for the system. On the other hand, if $\eta \leq 0$, then m^2 is given by the minus sign in (3.3). In this case the Mexican hat shape is lost for (3.2), so there is no Higgs-type potential and therefore no SSB. We must note that in both cases $m^2 > 0$, so the effective mass is always real. From this analysis, we define the critical temperature T_c for SSB to occur. This temperature is given in terms of η as $\eta(T_c) = 0$, so that

$$T_c \equiv \frac{2m_\Phi}{\sqrt{\lambda}}. \tag{3.4}$$

The SSB is then possible for temperatures in the range $T \in [0, T_c)$, while for $T \geqslant T_c$ there is no SSB. We are only interested in the case where there may be an SSB, so from now on we consider only temperatures $T < T_c$. Hence we take the plus sign on (3.3) and we can rewrite m^2 in terms of T and T_c as

$$m^2 = m_\Phi^2\left(1 - \frac{T^2}{T_c^2}\right). \tag{3.5}$$

The associated Higgs potential has a double minimum at $|\Phi|^2 \equiv \Phi\Phi^* = \frac{m^2}{\lambda}$. Then, the expected value of Φ at the vacuum can be expressed as

$$\langle\Phi\rangle_0 = \Phi_0 = \pm\frac{m}{\sqrt{\lambda}}. \tag{3.6}$$

We must note that the vacuum state depends on the effective mass m and hence on the temperature T that we consider for the thermal bath. This is noteworthy because it is this effective mass that we can use to impose constraints in the search for dark matter and comparisons with observables.

JCAP01(2024)018

Now, we put the potential (3.2) into the general Lagrangian (2.2), with m given by equation (3.5). In this case we can rewrite the complex scalar field Φ as excitations of the ground state Φ_0 (3.6) associated to the potential (3.2). So, using Polar notation, we decompose Φ in terms of two real scalar fields, $\rho(x)$ and $\theta(x)$, by doing radial perturbations around Φ_0 as follows

$$\Phi = [\Phi_0 + \rho(x)]\, e^{i\theta(x)}. \tag{3.7}$$

By substituting this expression of Φ in the general Lagrangian, only the terms of the covariant derivatives and of the potential V are modified, and by choosing the unitary gauge $\theta(x) = 0$ to break the symmetry of the ground state, then the Lagrangian $\mathcal{L}$ is now written as

$$\begin{aligned}\mathcal{L} = &-\frac{1}{4}F_{\mu\nu}F^{*\mu\nu} - \frac{1}{4}B_{\mu\nu}B^{*\mu\nu} - \frac{\delta^2}{2}R_e\left\{F_{\mu\nu}B^{\mu\nu}\right\} - \nabla^\mu\rho\nabla_\mu\rho - q^2\left(\Phi_0+\rho\right)^2 B_\mu B^{*\mu} - V(\rho) \\ &+ 2q\left(\Phi_0+\rho\right)\nabla_\mu\rho\,\mathrm{Im}\left\{B^\mu\right\},\end{aligned} \tag{3.8}$$

where

$$V(\rho) = \frac{\lambda}{2}\left\{4\Phi_0^2\rho^2 + 4\Phi_0\rho^3 + \rho^4\right\}. \tag{3.9}$$

As we can see, this Lagrangian already contains a mass term $q^2\Phi_0^2 B_\mu B^{*\mu}$ for the DP. So, now we can define the mass μ of the dark photon field as

$$\frac{1}{2}\mu^2 \equiv q^2\Phi_0^2 = q^2\frac{m^2}{\lambda}. \tag{3.10}$$

Therefore, in this model, the mass μ of the DP is limited by the self-interaction parameter λ, the effective mass m of the scalar field dark matter, and the gauge charge q. The Lagrangian (3.8) also contains a mass term $2\lambda\Phi_0^2\rho^2$ for the ρ field. This term is also known as Higgs mode, which, as we saw previously, is associated with radial perturbations of the ground state in the Higgs potential. The Higgs mode has an associated mass defined as $m_\rho \equiv \sqrt{2\lambda}\Phi_0 = \sqrt{2}m$. In order to decouple the ρ and B_μ fields and obtain a Proca-like Lagrangian from (3.8), we could in principle consider a Stueckelberg mechanism, which could be obtained in the case where $\lambda \gg q$ (so that the mass m_ρ of the Higgs mode is much larger than that of the dark photon μ). This process could be studied in the context of a UV completion theory for the Proca model, so that the Proca model is obtained at low effective energies. However, the Ly-alpha observations adjusted for self-interacting SFDM constrain the value of λ to be much less than 1 (of about 10^{-86} for ultralight scalar fields with masses of about $m_\Phi \sim 10^{-22}\,\mathrm{eV}$) in order to satisfy the constraints of nucleosynthesis [37]. While, in [33], the production of Fermi bubbles was studied using model (2.1), with values for q around $q \sim 10^{-13}$. Therefore, although it is interesting to explore both ranges ($\lambda > q$ and $\lambda < q$), what we can expect is that for SFDM models with ultra-light masses, λ is less than q. Due to this, the approximation that we use in this work is to consider regions where the scalar dark matter field Φ is quenched at its expected value in vacuum ($\Phi(x) = \Phi_0$), which is equivalent to considering that the radial perturbations of the ground state associated with the Higgs mode are negligible and therefore $\rho(x) = 0$. In this case, the Lagrangian (3.8) can be written simply as

$$\mathcal{L} = -\frac{1}{4}F_{\mu\nu}F^{*\mu\nu} - \frac{1}{4}B_{\mu\nu}B^{*\mu\nu} - \frac{1}{2}\mu^2 B_\mu B^{*\mu} - \frac{\delta^2}{2}R_e\left\{F_{\mu\nu}B^{\mu\nu}\right\}. \tag{3.11}$$

We should note that although up until now we have considered the case where A_μ and B_μ are complex, the discussion presented is still valid for the case where both are real, and is

JCAP01(2024)018

in this case when we recover the usual SSB process for the DP. So the Lagrangian (3.11) simply describes a dark photon with mass μ and a kinetic mixing parameter δ^2. From this Lagrangian, we can study the formation of Proca stars composed of dark photons, as has been previously done in the general case of spin-1 bosons. The difference in this case is that the DP acquires mass from its interaction with the SFDM, which imposes constraints on the mass of the dark photon. The approximation studied in this work also has the consequence that in places where there is SFDM, we could find not only massless dark photons, as described in [33], but also dark photons with mass, which can form astrophysically interesting objects.

4 Proca stars

As a first approximation we consider the case where there is no electromagnetic field of the SM (or it is negligible), so we can set $A_\mu = 0$. In this case (3.11) reduces to a Proca-type Lagrangian that we can write as

$$\mathcal{L}_{\rm P} = -\frac{1}{4} B_{\mu\nu} B^{*\mu\nu} - \frac{\mu^2}{2} B_\mu B^{*\mu}. \tag{4.1}$$

We couple this Lagrangian minimally with gravity and we obtain a Proca-Einstein action $S_{\rm P}$ of the form

$$S_{\rm P} = \int d^4x \sqrt{-g} \left[\frac{R}{16\pi G} + \mathcal{L}_{\rm P} \right]. \tag{4.2}$$

By varying this action with respect to the metric, we find the following Einstein equations

$$G_{\mu\nu} = 8\pi G \left[g_{\mu\nu} \mathcal{L}_{\rm P} - B_{\alpha(\mu} B^{*\alpha}_{\nu)} + 2\hat{U} B_{(\mu} B^{*}_{\nu)} \right], \tag{4.3}$$

and the variation with respect to B_μ gives Proca's equations of motion

$$\nabla_\mu B^{\mu\nu} = 2\hat{U} B^\nu, \tag{4.4}$$

where, following the same notation as in [16], we have defined a general potential $U\left(B^2\right) = \frac{1}{2}\mu^2 B_\mu B^{*\mu}$ (this notation is useful for the case in which self-interaction quartic potentials are considered for B_μ) and $\hat{U} \equiv \frac{dU}{dB^2}$, where $B^2 \equiv B_\mu B^{*\mu}$. This system has been arduously studied in a general way in [22] for spherical symmetric and static space-times and in [38] for the spinning case. In this work, we just consider the spherical symmetric and static case as a first approximation. We proceed in the same manner as in [16, 22] and propose a metric of the following form

$$dS^2 = -\sigma^2(r) N(r) dt^2 + \frac{dt^2}{N(r)} + r^2 d\Omega_2, \tag{4.5}$$

and for the dark photon field we propose a Proca-type ansatz of the form

$$B(r,t) = [f(r)dt + ig(r)dr] e^{-i\omega t}, \tag{4.6}$$

where $N(r) \equiv 1 - 2m(r)/r$; $\sigma(r)$, $m(r)$, $f(r)$ and $g(r)$ are real functions of the radial coordinate r, and ω is a real frequency parameter. We must be careful not to confuse the function $m(r)$ associated with the metric with the effective mass parameter m of the scalar field of

JCAP01(2024)018

dark matter, defined in (3.5) (which is a constant). Substituting the metric (4.5) and the ansatz (4.6) into equations (4.3), we obtain that the non-zero Einstein equations are [22]

$$m' = 4\pi G r^2 \left[\frac{(f' - \omega g)^2}{2\sigma^2} + \frac{\mu^2}{2} \left(g^2 N + \frac{f^2}{N\sigma^2} \right) \right], \tag{4.7}$$

$$\frac{\sigma'}{\sigma} = 4\pi G r \mu^2 \left(g^2 + \frac{f^2}{N^2\sigma^2} \right), \tag{4.8}$$

while the Proca equations (4.4) are

$$\frac{d}{dr} \left\{ \frac{r^2 \left[f' - \omega g \right]}{\sigma} \right\} = \frac{\mu^2 r^2 f}{\sigma N}, \tag{4.9}$$

$$\omega g - f' = \frac{\mu^2 \sigma^2 N g}{\omega}, \tag{4.10}$$

where the $'$ indicates derivation with respect to the radial coordinate r. This system can be solved numerically. We can do expansions at $r \to \infty$ and $r \to 0$, as in [22], in order to investigate the behavior of the functions and propose pertinent boundary conditions to solve the system. The maximal ADM mass $M_{\rm ADM}$ of this type of solution is given in terms of the dark photon mass μ by the following relation [39]

$$M_{\rm ADM}^{\rm max} = \alpha_{\rm BS} \frac{M_{\rm Pl}^2}{\mu} = \alpha_{\rm BS} 1.34 \times 10^{-19} M_\odot \frac{\rm GeV}{\mu}, \tag{4.11}$$

where $M_{\rm Pl}$ is the Planck's mass, and $\alpha_{\rm BS}$ is a constant numerical parameter which is set to $\alpha_{\rm BS} = 1.058$ for static and spherically symmetric metrics [39]. Using the definition (3.10) of μ we can write $M_{\rm ADM}$ in terms of m, q and λ as

$$M_{\rm ADM}^{\rm max} = \alpha_{\rm BS} 1.34 \times 10^{-19} M_\odot \frac{\sqrt{\lambda}}{\sqrt{2} q m} \, \text{GeV}. \tag{4.12}$$

In figures 1 and 2, we plot the maximal ADM mass $M_{\rm ADM}^{\rm max}$ for different values of λ and q. From figure 1, we can observe that for a fixed $\lambda = 10^{-50}$ and an effective mass of the scalar field of $m = 10^{-24}\, eV$, the maximal mass $M_{\rm ADM}$ of the Proca star reaches values of astrophysical relevance when $q < 10^{-8}$, while for larger values of q, the masses are considerably smaller than a solar mass. On the other hand, if we fix $q = 10^{-15}$ now, from figure 2 we can observe that $M_{\rm ADM}$ increases for large values of λ. However, due to the constraints of Ly-alpha observations adjusted for self-interacting SFDM studied in [37], we know that for ultra-light effective masses of self-interacting scalar fields, the self-interaction parameter λ must be very small (but different from zero). In figure 2, we consider values of $\lambda \sim 10^{-51}$ that, although not as small as predicted in [37], can be considered within the physical range of SFDM. Therefore, we can conclude that, as expected, the λ, m, and q parameters of the SFDM field strongly influence the mass of the associated dark photons, and thus also affect the masses of the Proca stars obtained from this system.

5 Proca stars and dark photon

We now consider the case where the electromagnetic field of the SM is not negligible. In this case, the nature of the DP and its interaction with the SM photon becomes manifest, so we

JCAP01(2024)018

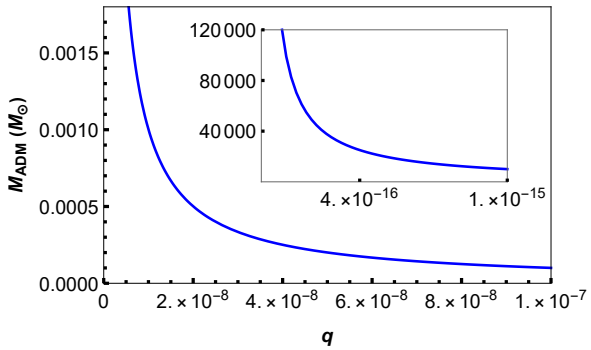

Figure 1. Maximal ADM mass for different values of the gauge charge q with $\lambda = 10^{-50}$ and $m = 10^{-24}\,\mathrm{eV}$.

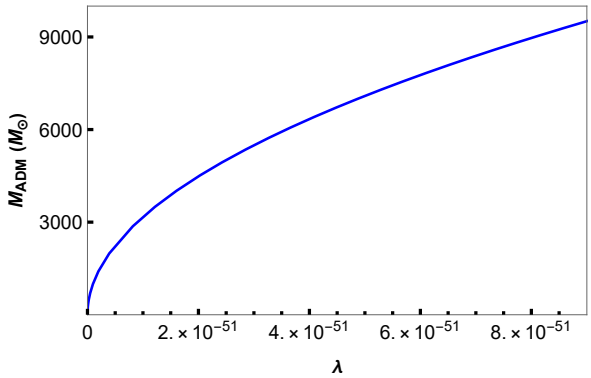

Figure 2. Maximal ADM mass for different values of the self-interaction parameter λ of the SFDM field with $q = 10^{-15}$ and $m = 10^{-24}\,\mathrm{eV}$.

consider the Lagrangian (3.11), which from now on we call $\mathcal{L}_{\mathrm{DP}}$, so that

$$\mathcal{L}_{\mathrm{DP}} = -\frac{1}{4}F_{\mu\nu}F^{*\mu\nu} - \frac{1}{4}B_{\mu\nu}B^{*\mu\nu} - U\left(B^2\right) - \frac{\delta^2}{2}R_e\left\{F_{\mu\nu}B^{\mu\nu}\right\}, \tag{5.1}$$

where $U\left(B^2\right)$ is defined the same as in the previous section. Following the same analysis as in the case of Proca, we find that the action for the system is given by $S_{\mathrm{DP}} = \int\left[\frac{1}{16\pi G}R + \mathcal{L}_{\mathrm{DP}}\right]\sqrt{-g}d^4x$. The variation of this action with respect to the metric leads us to the following Einstein equations

$$G_{\mu\nu} = 8\pi G\left(g_{\mu\nu}\mathcal{L}_{\mathrm{DP}} - F_{\alpha(\mu}F^{*\alpha}_{\nu)} - B_{\alpha(\mu}B^{*\alpha}_{\nu)} + 2\hat{U}B_{(\mu}B^{*}_{\nu)} - \delta^2\left[F_{\alpha(\mu}B^{\alpha}_{\nu)} + F^{*}_{\alpha(\mu}B^{*\alpha}_{\nu)}\right]\right). \tag{5.2}$$

While varying A_μ and B_μ we obtain the following equations of motion for the fields. Varying A_μ we have

$$\nabla_\mu\left(F^{\mu\nu} + \delta^2 B^{*\mu\nu}\right) = 0, \tag{5.3}$$

and varying B_μ we have

$$\nabla_\mu\left(B^{\mu\nu} + \delta^2 F^{*\mu\nu}\right) = 2\hat{U}B^{\nu}. \tag{5.4}$$

From these field equations we observe that for the case where the kinetic mixing parameter is $\delta^2 = 0$, the Maxwell and Proca electrodynamics are recovered for the fields A_μ and B_μ

JCAP01(2024)018

respectively, which was to be expected. The equations (5.3) and (5.4) also imply the modified Lorentz condition for the DP field B_μ

$$\nabla_\nu \left(\hat{U} B^\nu\right) = 0, \tag{5.5}$$

so now this is a dynamical requirement. While for the SM photon field A_μ we are free to choose the gauge fixing, which we decide to be also a Lorentz gauge condition

$$\nabla_\nu \left(A^\nu\right) = 0. \tag{5.6}$$

The system (5.1) possesses an U(1) global invariance of the form $B_\nu \to e^{i\alpha} B_\nu$, with $A_\nu \to e^{-i\alpha} A_\nu$, where α is a real constant. This implies that there is a conserved 4-current J^μ, which we have split as $J^\mu = J^\mu_B + J^\mu_{AB}$, where we have defined

$$\begin{aligned} J^\mu_B &\equiv \frac{i}{2}\left\{B_\nu B^{*\mu\nu} - B^*_\nu B^{\mu\nu}\right\}, \\ J^\mu_{AB} &\equiv \frac{i}{2}\left\{A^*_\nu F^{\mu\nu} - A_\nu F^{*\mu\nu}\right\} + \delta^2 \,\mathrm{Im}\left\{A_\nu B^{\mu\nu} - B_\nu F^{\mu\nu}\right\}, \end{aligned} \tag{5.7}$$

we can see that J^μ_B corresponds to the usual 4-current for the Proca field, while J^μ_{AB} corresponds to the 4-current for the SM photon field A_μ plus the cross terms between A_μ and B_μ. As we can see, the cross terms in the current disappear as δ^2 becomes zero. Finally, from (5.3) and (5.4) we have $\nabla_\mu J^\mu = 0$, so there exist a total Noether charge Q defined as $Q = \int_\Sigma d^3x\sqrt{-g}J^t$. In the same way, it can be shown from (5.7), (5.3) and (5.4) that $\nabla_\mu J^\mu_B = \nabla_\mu J^\mu_{AB} = 0$, so we may write the total Noether charge Q as

$$Q = Q_B + Q_{AB}, \tag{5.8}$$

where we have defined $Q_B \equiv \int_\Sigma d^3x\sqrt{-g}J^t_B$, and $Q_{AB} \equiv \int_\Sigma d^3x\sqrt{-g}J^t_{AB}$. These charges are convenient ways to rewrite the total Noether charge Q associated with the global U(1) symmetry of the system.

To find solutions to the system, we again consider a static and spherically symmetric metric like the one proposed in (4.5) and, inspired by Proca's ansatz [22], we propose that A_μ and B_μ are of the following form

$$B = e^{-i\omega t}[f(r)dt + ig(r)dr], \tag{5.9}$$

$$A = e^{i\omega t}[h(r)dt - ij(r)dr], \tag{5.10}$$

where, as in the case of Proca, $f(r)$, $g(r)$, $h(r)$ and $j(r)$ are real functions that only depend on the radial coordinate, while ω is a frequency parameter. It's important to note that we are using the same frequency parameter ω for the time evolution of both fields. This is proposed in this way just to be able to obtain a time-independent system of differential equations after we substitute the ansatz in the Einstein equations and field equations of motion; otherwise, we could not find a time-independent system, at least with this ansatz. Substituting these forms of A_μ, B_μ and the metric (4.5) we obtain that the non-zero Einstein equations are

$$m' = 4\pi G r^2 \left\{\mu^2\left[\frac{Ng^2}{2} + \frac{f^2}{2N\sigma^2}\right] + \frac{1}{2\sigma^2}\left[(\omega g - f')^2 + 2\delta^2\left(wg - f'\right)\left(\omega j - h'\right) + \left(wj - h'\right)^2\right]\right\}, \tag{5.11}$$

$$\frac{\sigma'}{\sigma} = 4\pi G r \mu^2\left[g^2 + \frac{f^2}{N^2\sigma^2}\right]. \tag{5.12}$$

JCAP01(2024)018

The field equations resulting from varying B_μ are

$$\frac{d}{dr}\left\{\frac{r^2}{\sigma}\left[(f'-\omega g)+\delta^2\left(h'-\omega j\right)\right]\right\}=\frac{r^2\mu^2 f}{\sigma N}, \tag{5.13}$$

$$(\omega g-f')+\delta^2\left(\omega j-h'\right)=\frac{\mu^2\sigma^2 g N}{\omega}, \tag{5.14}$$

and the field equations resulting from varying A_μ are

$$\frac{d}{dr}\left\{\frac{r^2}{\sigma}\left[(h'-\omega j)+\delta^2\left(f'-\omega g\right)\right]\right\}=0, \tag{5.15}$$

$$h'-\omega j=-\delta^2\left(f'-\omega g\right). \tag{5.16}$$

Thus, in principle we have a system of 6 differential equations with 6 functions to determine. Note, however, that the penultimate equation (5.15) holds trivially because of the last (5.16). Furthermore we can see that by substituting the equation (5.16) into the first 4 equations (5.11)–(5.14), we can eliminate the functions $j(r)$ and $h(r)$ from these equations. Then the system is reduced to 5 equations with 6 functions to determine. Now Einstein's equations can be written as

$$m'=4\pi G r^2\left[\frac{\left(1-\delta^4\right)\left(f'-\omega g\right)^2}{2\sigma^2}+\frac{\mu^2}{2}\left(g^2N+\frac{f^2}{N\sigma^2}\right)\right], \tag{5.17}$$

$$\frac{\sigma'}{\sigma}=4\pi G r\mu^2\left(g^2+\frac{f^2}{N^2\sigma^2}\right), \tag{5.18}$$

and the field equations in this case reduce to

$$\frac{d}{dr}\left\{\frac{r^2\left[f'-\omega g\right]}{\sigma}\right\}=\frac{\mu^2 r^2 f}{\sigma N(1-\delta^4)}, \tag{5.19}$$

$$\omega g-f'=\frac{\mu^2\sigma^2 N g}{\omega(1-\delta^4)}, \tag{5.20}$$

$$h'-\omega j=-\delta^2\left(f'-\omega g\right). \tag{5.21}$$

We can see that the first 4 equations (5.17)–(5.20) of this new system simply correspond to a system of equations of the type Einstein-Proca as obtained in the Proca stars section above, except for a constant term $(1-\delta^4)$ that multiplies the equations. The constraints for δ are $\delta^2\neq 1;\delta^2\leqslant 10^{-6}$ [40] (because very weak interactions are requested between both photons), therefore $(1-\delta^4)\neq 0$ and the system is well defined. While the functions $h(r)$ and $j(r)$ that describe the field of the SM photon are defined in terms of those of the dark photon $f(r)$ and $g(r)$ through the equation (5.21). To close the system we can consider a gauge fixing for A_μ, such as the Lorentz condition $\nabla_\mu A^\mu=0$ (which is a requirement and not a choice for the case of B_μ [22]). In this case, considering the ansatz (5.10) and the metric (4.5), the Lorentz condition for A_μ can be written as

$$\frac{d}{dr}\left\{\frac{\sigma j r^2 N}{\omega}\right\}=\frac{-r^2 h}{\sigma N}. \tag{5.22}$$

JCAP01(2024)018

In the same way, using the ansatz (5.9), (5.10) and (4.5) the total Noether charge Q, and the charges Q_A and Q_{AB} read in this case as

$$\begin{aligned} Q &= \frac{4\pi\mu^2}{\omega}\int_0^\infty drr^2g^2\sigma N, \\ Q_B &= \frac{4\pi\mu^2}{\omega\left(1-\delta^4\right)}\int_0^\infty drr^2g^2\sigma N, \\ Q_{AB} &= \frac{-4\pi\mu^2\delta^4}{\omega\left(1-\delta^4\right)}\int_0^\infty drr^2g^2\sigma N, \end{aligned} \tag{5.23}$$

so for this ansatz, we have the interesting special case of $Q_{AB} = -\delta^4 Q_B$, and therefore the total Noether charge Q can be written as $Q = \left(1-\delta^4\right)Q_B$.

On the other hand, we can calculate the Komar mass $M_{\rm K}$ associated with the system by considering the following integral

$$M_{\rm K} = 2\int_\Sigma \left(T_{ab} - \frac{1}{2}Tg_{ab}\right)n^a\xi^b dV, \tag{5.24}$$

where Σ is an asymptotically-flat spacelike hypersurface, n^a is the unit future pointing normal to Σ, and dV is the natural volume element on Σ. So, the Komar mass for the ansatz (5.10), (5.9) and (4.5) is given by

$$M_{\rm K} = 4\pi\int_0^\infty dr\frac{r^2}{\sigma N}\left[\left(f'-\omega g\right)^2\left(1-\delta^4\right)N + 2f^2\mu^2\right]. \tag{5.25}$$

Finally, we follow the analysis presented in [41–43] to find that the Lagrangian (5.1) must obey a virial identity of the form

$$\int_0^\infty drr^2\sigma\left[\mu^2\left(g^2 - \frac{f^2(4N-1)}{\sigma^2N^2}\right) - \frac{\left(f'-wg\right)^2\left(1-\delta^4\right)}{\sigma^2}\right] = 0. \tag{5.26}$$

In order to assess the quality of our numerical solutions, we can verify that the virial identity is satisfied, as well as compare the Komar mass obtained from (5.25) with the ADM mass M calculated by evaluating the mass function $m(r)$ at the numerical infinity.

In order to find the solutions for the functions that describe the system, we must simultaneously solve the equations (5.17)–(5.22). In the next section we solve the system numerically for the non-asymptotic regions, and we study graphically how the solutions for each function are modified. We are particularly interested in the functions $j(r)$ and $h(r)$ that describe the photon of the SM, since, in principle, it is from these functions that observations could be obtained.

6 Results

To preserve the regularity of the system of equations at the origin, it is necessary to consider series expansions for the functions around $r = 0$, so that [22, 44]

$$\begin{aligned} f(r) &= f_0 + \mathcal{O}\left(r^2\right), \\ g(r) &= \mathcal{O}(r), \end{aligned}$$

JCAP01(2024)018

$$
\begin{aligned}
m(r) &= \mathcal{O}\left(r^3\right), \\
\sigma(r) &= \sigma_0 + \mathcal{O}\left(r^2\right), \\
h(r) &= h_0 + \mathcal{O}\left(r^2\right), \\
j(r) &= \mathcal{O}(r),
\end{aligned}
\tag{6.1}
$$

where $\sigma(0) = \sigma_0$, $f(0) = f_0$ and $h(0) = h_0$ are the boundary conditions at the origin. Additionally, to preserve the asymptotic flatness, it is necessary that the mass functions f and g of the dark photon decay exponentially at infinity, therefore

$$
f(\infty) = g(\infty) = 0. \tag{6.2}
$$

While the functions N and σ of the metric must approach 1 at infinity. Therefore we impose

$$
m(\infty) = M, \quad \sigma(\infty) = 1, \tag{6.3}
$$

where M is the total mass of the star, which can be identified as the ADM mass of the system. Finally, for the electromagnetic field of the SM photon, we can consider constant electric and magnetic potentials at infinity

$$
h(\infty) = h_\infty, \quad j(\infty) = j_\infty, \tag{6.4}
$$

where h_∞ and j_∞ are constants that, in this case, we fix equal zero in order to satisfy the asymptotic behavior of the system of differential equations (5.17)–(5.22). By analyzing the asymptotic behavior of the system, we find that as $r \to \infty$, the functions allow expansions of the form

$$
\begin{aligned}
f(r) &= \frac{c_0 e^{-r\sqrt{\frac{\mu^2}{1-\delta^4}-\omega^2}}}{r} + \ldots, \\
g(r) &= \frac{c_0 \omega e^{-r\sqrt{\frac{\mu^2}{1-\delta^4}-\omega^2}}}{r\sqrt{\frac{\mu^2}{1-\delta^4}-\omega^2}} + \ldots, \\
h(r) &= -\frac{c_0 \delta^2 e^{-r\sqrt{\frac{\mu^2}{1-\delta^4}-\omega^2}}}{r} + \frac{c_1 \cos(\omega r)}{r} + \frac{c_2 \sin(\omega r)}{2r\omega} + \ldots, \\
j(r) &= -\frac{c_0 \omega \delta^2 e^{-r\sqrt{\frac{\mu^2}{1-\delta^4}-\omega^2}}}{r\sqrt{\frac{\mu^2}{1-\delta^4}-\omega^2}} + \frac{c_2 \cos(\omega r)}{2r\omega} - \frac{c_1 \sin(\omega r)}{r} + \ldots, \\
m(r) &= M + \ldots, \\
\log\sigma(r) &= -\frac{4\pi G \mu^4 c_0^2 e^{-2r\sqrt{\frac{\mu^2}{1-\delta^4}-\omega^2}}}{2\left(1-\delta^4\right) r \left(\frac{\mu^2}{1-\delta^4}-\omega^2\right)^{3/2}} + \ldots,
\end{aligned}
\tag{6.5}
$$

where c_0, c_1 and c_2 are constants. We observe from these expansions that now the bound state condition for Proca stars is modified in terms of the kinetic mixing parameter δ^2, and

JCAP01(2024)018

now reads

$$\omega < \frac{\mu}{\sqrt{1-\delta^4}}. \tag{6.6}$$

These expansions also introduce condition $(1-\delta^4) > 0$, which is compatible with the physical constrictions of δ^2 for the DP.

The numerical results are calculated using the rescaled quantities $r \to \mu r$, $m \to \mu m$, $\omega \to \omega/\mu$ and the rescaled potentials $f \to \sqrt{4\pi G} f$, $g \to \sqrt{4\pi G} g$, $h \to \sqrt{4\pi G} h$, and $j \to \sqrt{4\pi G} j$. In addition to these rescalings, the system also possesses the following symmetry

$$\{\sigma, \omega, f_0, h_0\} \to \xi \{\sigma, \omega, f_0, h_0\}, \tag{6.7}$$

where ξ is fixed in such a way that $\sigma(\infty) = 1$.

To solve the system we use "NDSolve" command in *Mathematica* and evaluate the initial conditions at $r = 10^{-6}$. We can vary f_0 in analogy to a shooting method and set σ_0 and M numerically. To calculate the branches of M and Q as a function of ω, we followed the same process, but we adapted the *Mathematica* Notebook for boson stars made by Macedo et al., mentioned in [45], for our system. In all cases, we fix the commands *AccuracyGoal* $\to$ 13 and *PrecisionGoal* $\to$ 12 for NDSolve. Using the virial equation, we found an estimated error of the order of 10^{-2}–10^{-7} in the solutions. While comparing the Komar mass with the ADM mass, we found a difference of less than 1% in all solutions. We attribute a part of the numerical error to the fact that the code implements a logarithmic step succession; however, we also found that the error increases for relatively high δ values, such as $\delta > 0.5$. We think that this error may be due to the indeterminacy of the system of differential equations as δ approaches 1 due to factors of $(1-\delta^4)$ in the denominator.

In figures 3 and 4, we use approximately the same values for the parameters as in figure 2 in [22] to compare how the Proca case solutions differ due to the presence of the SM photon. In both figures, we take $\delta^2 \sim 10^{-14}$ based in the Ly-alpha observations adjusted for dark photons in reference [46]. We must remark that in figures 3 and 4, as well as in all the results presented in this paper, the family of solutions for the function $f(r)$ possesses one node, while the solutions for $g(r)$ are nodeless, just as in the case of the mini Proca stars studied in [22].

As we can observe, the functions $m(r)$ and $\sigma(r)$ of the metric and the functions $f(r)$ and $g(r)$ of the dark photon vary very little from the case where $\delta^2 = 0$ (the pure Proca case presented in [22]). This is to be expected due to the δ^4 factor in the differential equations. In fact, at a given numerical radius, R, the variations of the numerical solutions for the functions $m(r)$ and $\sigma(r)$ when $\delta^2 = 0$ and when $\delta^2 \sim 10^{-14}$ are of the order of $m(\delta^2 = 0) - m(\delta^2 = 10^{-14}) \sim 10^{-7}$. Variations in these functions become noticeable until the kinetic mixing parameter δ^2 takes on values so large that they are outside of the physical ultralight DP range. In figure 5, for example, we take $\delta^2 > 10^{-3}$; in these cases, the changes in the mass function $m(r)$ for the star become considerable, and therefore changes in the maximal ADM mass could be expected; however, taking values of δ in the physical range, these differences become increasingly negligible. The solutions for the functions $g(r)$, $f(r)$, $j(r)$, and $h(r)$ present similar behavior with respect to the variations in δ^2.

On the other hand, due to the way the functions are coupled in the system of differential equations, we know that the initial values f_0 and σ_0 strongly determine the behavior of the metric and DP functions, while the initial value h_0 of the SM photon has a weak influence on these functions. In fact, by varying h_0 as shown in figure 6, the difference between the numerical solutions for the functions $f(r)$, $g(r)$, $\sigma(r)$, and $m(r)$ at a given numerical radius R is of the order of $\sim 10^{-6}$. This suggests that the SM photon has a relatively small effect on

JCAP01(2024)018

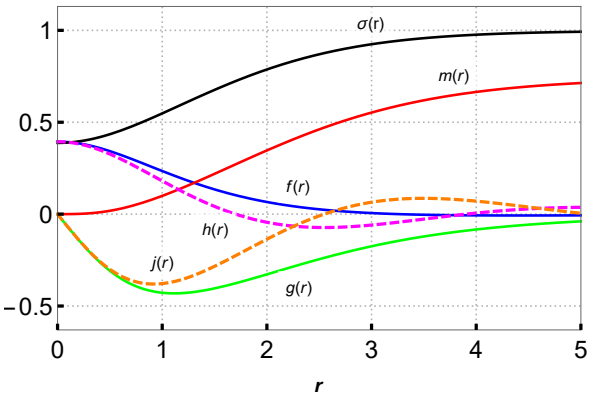

Figure 3. Numerical solutions for the functions $m(r)$ (red), $\sigma(r)$ (black), $f(r)$ (blue), $g(r)$ (green), $h(r)$ (dashed magenta), and $j(r)$ (dashed orange) are obtained with fixed $M = 0.745$, $\omega = 0.817$, $f_0 = h_0 = 0.394$, and $\delta^2 = 10^{-14}$.

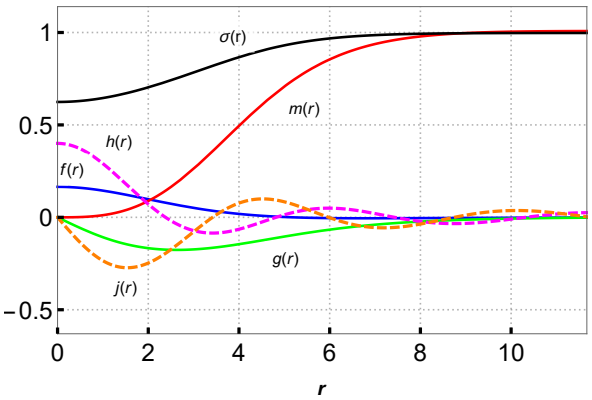

Figure 4. Numerical solutions for the functions $m(r)$ (red), $\sigma(r)$ (black), $f(r)$ (blue), $g(r)$ (green), $h(r)$ (dashed magenta), and $j(r)$ (dashed orange) are obtained with fixed $M = 1.016$, $\omega = 0.839$, $f_0 = 0.165$, $h_0 = 0.4$ and $\delta^2 = 10^{-14}$.

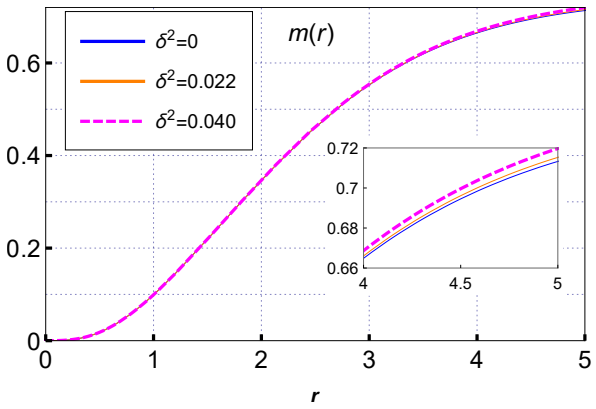

Figure 5. Numerical solutions for the function $m(r)$ are obtained for different values of δ^2 with fixed $\omega = 0.817$, and $f_0 = h_0 = 0.394$.

JCAP01(2024)018

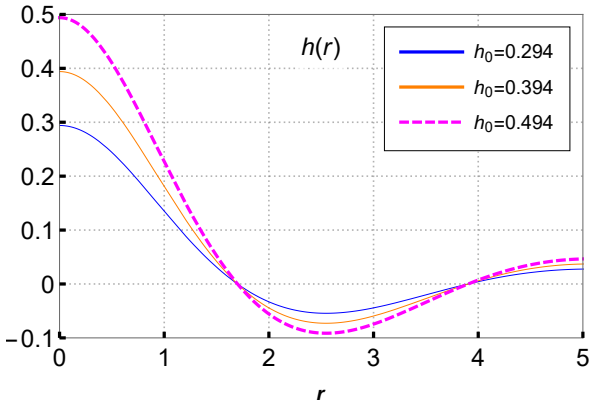

Figure 6. Numerical solutions for the function $h(r)$ are obtained for different values of h_0 with fixed $M = 0.745$, $\omega = 0.817$, $f_0 = 0.394$, and $\delta^2 = 10^{-14}$.

the behavior of the other functions in the system and that it may be possible to neglect it in certain cases. However, the choice of h_0 strongly influences the functions of the SM photon $j(r)$ and $h(r)$. Therefore, we can vary h_0 to fix the values of $j(r)$ and $h(r)$ at infinity without significantly modifying the metric and DP functions. This would allow us, in principle, to vary h_0 to adjust the observables of the electromagnetic field of the SM photon associated with a Proca-like star.

In figure 7 we plot the ADM mass M and the charge Q_B as functions of ω for a relatively large value of $\delta^2 = 0.25$ in order to observe the behavior of the branch. At first glance, we can see that the maximum value allowed for ω in this case does not tend to 1 but tends to $\frac{1}{\sqrt{1-\delta^4}} \approx 1.032$, this is due to the modified bound condition (6.6) found from the asymptotic expansions for the system. This same behavior is exhibited by the other branches of M and Q_B for different values of δ^2. In each of these branches, we observe that as $\omega \to \frac{1}{\sqrt{1-\delta^4}}$, M and Q_B tend to zero, with $M/Q_B \to 1$. Which corresponds to a behavior analogous to mini PS. In the same way, in all the solutions, the spiral behavior of M and Q_B is maintained around a central value of ω, which varies for each branch of δ^2. From figure 7, we can also see that there are still two regions, one where $M > Q_B$ and another where $M < Q_B$. Both regions are divided by a point close to the minimum value of ω. On the other hand, from figure 8, we can explicitly see the shift of the maximum value of ω for each branch of M for different values of δ^2. We see that the greater the δ^2, the greater the shift in the branch of M, and the smaller the δ^2, the closer it is to the case of mini PS. In order to compare the maximal ADM mass $M_{\rm ADM}^{\rm max}$ in each case, we can use symmetry (6.7) of the system and define an auxiliary $\widetilde{\omega}$ of the form

$$\widetilde{\omega} \equiv \omega\sqrt{1-\delta^4}. \tag{6.8}$$

Always keep in mind that ω is the physical numerical frequency fixed by the asymptotic condition $\sigma(\infty) = 1$, while $\widetilde{\omega}$ is just an auxiliary frequency to better visualize the graphs. Figure 9 shows exactly the same branches as in figure 8 but as a function of $\widetilde{\omega}$, so the shift in the branches of M has disappeared. From this figure we can see that the higher the δ^2 value, the smaller the maximal ADM mass $M_{\rm ADM}^{\rm max}$ reached by the branch, where the highest maximal mass is possessed by the $\delta^2 = 0$ branch with a maximal ADM mass $M_{\rm ADM}^{\rm max} = 1.0582$ (corresponding to mini PS case), while the smallest value of maximal ADM mass is found for $\delta^2 = 0.25$, with a maximal ADM mass of $M_{\rm ADM}^{\rm max} = 0.998$. As we can see from table 1, the branches of Q_B exhibit similar behavior.

JCAP01(2024)018

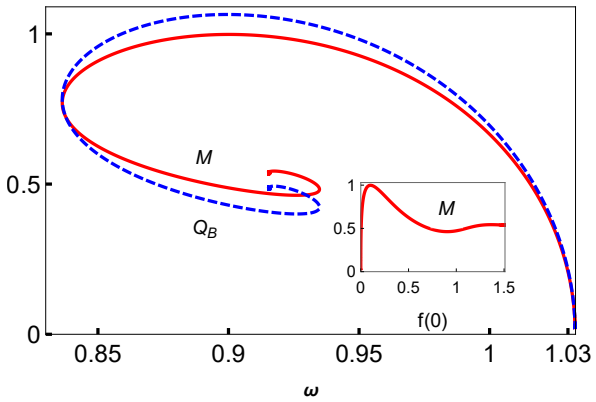

Figure 7. ADM mass M and charge Q_B vs. the frequency parameter ω, for a fixed $\delta^2 = 0.25$. The inset corresponds to M vs. the shooting parameter $f(0)$.

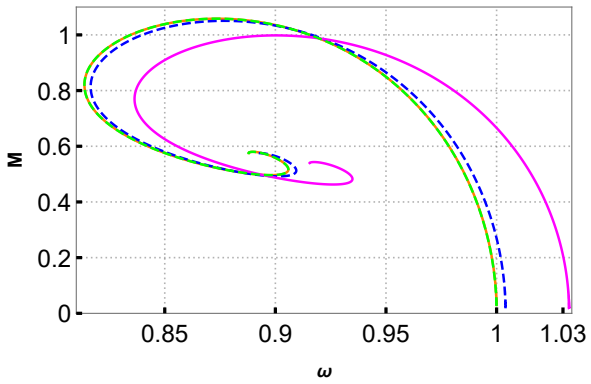

Figure 8. ADM mass M vs. the frequency parameter ω, for $\delta^2 = 0$ (dashed green), $\delta^2 = 0.01$ (orange), $\delta^2 = 0.09$ (dashed blue), and $\delta^2 = 0.25$ (magenta).

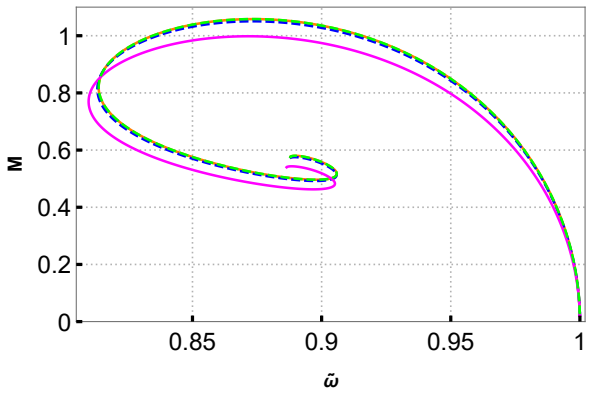

Figure 9. ADM mass M vs. the auxiliary frequency parameter $\widetilde{\omega}$, for $\delta^2 = 0$ (dashed green), $\delta^2 = 0.01$ (orange), $\delta^2 = 0.09$ (dashed blue), and $\delta^2 = 0.25$ (magenta).

In table 1, we list the maximal ADM mass $M_{\rm ADM}^{\rm max}$ for each value of δ^2. Here $\omega_{\rm max}$ and $\tilde{\omega}_{\rm max}$ correspond to the frequency values associated with $M_{\rm ADM}^{\rm max}$; $Q_{B\,\rm max}$ is the maximal value of Q_B, which also corresponds to $\omega_{\rm max}$ and $\tilde{\omega}_{\rm max}$, and $M_{\rm Komar}$ is the Komar mass

JCAP01(2024)018

	$\omega_{\max}$	$\tilde{\omega}_{\max}$	$M_{\rm ADM}^{\max}$	$Q_{B\,\max}$	$M_{\rm Komar}$
$\delta^2 = 0.00$	0.873	0.873	1.0582	1.0881	1.0582
$\delta^2 = 0.01$	0.873	0.873	1.0581	1.0880	1.0581
$\delta^2 = 0.09$	0.877	0.873	1.0504	1.085	1.0508
$\delta^2 = 0.25$	0.900	0.871	0.998	1.0645	1.0013

Table 1. Proca stars for different values of δ^2.

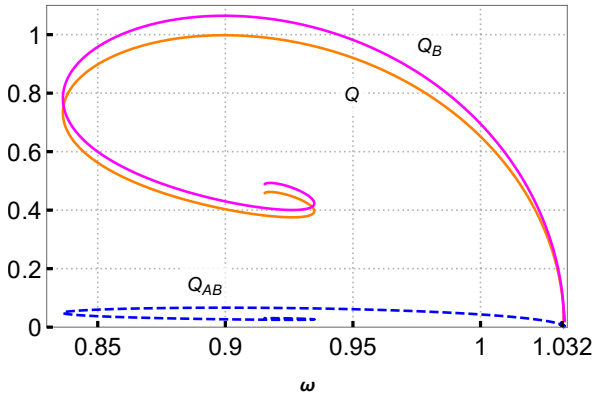

Figure 10. Noether charge Q (orange) and charges Q_B (magenta) and $|Q_{AB}|$ (dashed blue) vs. the frequency parameter ω, for a fixed $\delta^2 = 0.25$.

associated with $\omega_{\max}$. From table 1, we can also see that $\tilde{\omega}_{\max}$ is approximately the same for all δ^2 values. Finally, it should be noted that for δ^2 values less than 0.01, the changes in the parameters M, Q_B, and ω vary very little with respect to the case of $\delta^2 = 0$ corresponding to mini PS; therefore, for very small δ^2 values, it is possible that a substantial difference will not be noticed. However, although the parameters of the Proca star show very small changes, we can still measure the observables associated with the electromagnetic field of the SM photon A_μ, as we do in the next section. Finally, in figure 10, we plot the total Noether charge Q and the charges Q_B and $|Q_{AB}|$ as a function of the frequency parameter ω for the same $\delta^2 = 0.25$ value. The difference between the branches in this case is given by the proportionality factors $Q_{AB} = -\delta^4 Q_B$ and $Q = (1 - \delta^4)\, Q_B$, described in (5.23), which are valid for our ansatz (5.9), (5.10) and (4.5). As we can see, in this case, the Q_B charge is always the largest, and, as expected from its definition (5.7), it is the one that comes closest to the curve for the Noether charge of the mini PS case. As δ^2 approaches zero, $|Q_{AB}|$ goes to zero, while Q and Q_B become the same curve that corresponds to the Noether charge for mini PS.

7 Observables

Due to the form of the ansatz (5.10) for A_μ, the solutions are associated with a system with zero magnetic field $\bar{B} = 0$ and an electric field $\bar{E}$ given in terms of the electromagnetic tensor $F_{\mu\nu}$ as follows

$$E_i = F_{i0}, \tag{7.1}$$

where $i = \{r, \theta, \phi\}$, so that

$$\bar{E} = \left[h'(r) - \omega j(r)\right] e^{i\omega t} \hat{r}, \tag{7.2}$$

JCAP01(2024)018

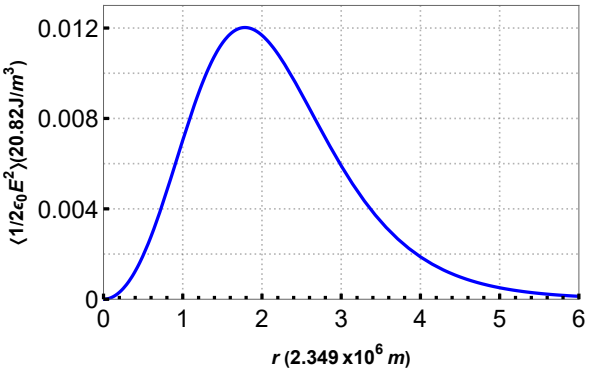

Figure 11. The expected value for the volumetric energy density of the electric field E is obtained for a solution with $\mu = 8.4 \times 10^{-14}$ and $\delta^2 = 4.6 \times 10^{-15}$.

where $\hat{r}$ is the unit vector in the radial direction. Therefore, the physical electric field is given by

$$\mathrm{Re}\{\bar{E}\} = [h'(r) - wj(r)]\cos(wt)\hat{r}, \tag{7.3}$$

and from now on we change the notation for the electric field to $\bar{E} \to \mathrm{Re}\{\bar{E}\}$. From here, we can calculate the expected value of the volumetric energy density associated with this electric field, given by

$$\left\langle \frac{1}{2}E^2 \right\rangle = \frac{1}{4}\left[h'(r) - wj(r)\right]^2. \tag{7.4}$$

In order to use the numerical solutions calculated in the previous section, it is necessary to return to the non-scaled functions. Therefore, in natural units, the electric field can be written in terms of the numerical solutions as follows

$$\left\langle \frac{1}{2}E^2 \right\rangle = \frac{\mu^2}{16\pi G}\left[h'_{(\mathrm{num})} - w_{(\mathrm{num})}j_{(\mathrm{num})}\right]^2. \tag{7.5}$$

Finally, in order to avoid numerical noise, we can use equation (5.21) to rewrite $h(r)$ and $j(r)$ in terms of $f(r)$ and $g(r)$, and directly introduce the δ^4 factor in the previous equation, so that

$$\left\langle \frac{1}{2}E^2 \right\rangle = \frac{\mu^2\delta^4}{16\pi G}\left[f'_{(\mathrm{num})} - w_{(\mathrm{num})}g_{(\mathrm{num})}\right]^2. \tag{7.6}$$

In figure 11, we present the density plot for numerical solutions with fixed values of $M = 0.745$, $\omega = 0.817$, $f_0 = h_0 = 0.394$, and $\delta^2 = 4.6 \times 10^{-15}$. We then return to the non-scaled functions by using a value of $\mu = 8.4 \times 10^{-14}\,\mathrm{eV}$ (motivated by the simulations made in [46] for DP) and express the results in SI units. For these specific parameter values, we obtain a maximum for the volumetric energy density at approximately $0.24\,\mathrm{J/m^3}$. As we can observe, due equation (7.6), the expected value of the volumetric energy density of the electric field strongly depends on the chosen value of δ^2. This energy decays to zero at infinity, as expected. In principle, it is this electric field and this density that we can use to adjust observations in the regions where Proca stars associated with dark photons are expected to be found. We hope to use this observable in future works to adjust real observational data.

One last important consideration to take into account is that, given the form of the complex electric field of the SM (7.2), we can once again use equation (5.21) to rewrite (7.2) as

$$\bar{E} = \left[h'(r) - \omega j(r)\right]e^{i\omega t}\hat{r} = \delta^2\left[\omega g(r) - f'(r)\right]e^{i\omega t}\hat{r}. \tag{7.7}$$

JCAP01(2024)018

From here, we observe that in the limiting case of $\delta = 0$, we obtain that the complex electric field of the SM is equal to zero (as well as the magnetic field of the SM due to the form of the ansatz, as we mentioned before). Then, we can conclude that in the case of $\delta = 0$, the electromagnetic field of the SM disappears, leaving only the Proca field of the dark photon as the only contributor to the formation of the Proca star, consistent with the results of the previous section, where for $\delta = 0$, we obtain the pure Proca case. However, it is important to note that having $\bar{E} = \bar{B} = 0$ when $\delta = 0$ does not imply that the potentials $h(r)$ and $j(r)$ are necessarily equal to zero. Actually, what happens in this limiting case is that the solutions for $h'(r)$ and $\omega j(r)$ are equal to each other, so it is true that $[h'(r) - \omega j(r)] = 0$. This behavior of the SM photon potentials can be appreciated directly in their expansions at $r \to \infty$, given by (6.5). First, we can use equations (6.5) to write the asymptotic expansion for the spatial part of the magnitude of $\bar{E}$ at $r \to \infty$ for any value of δ (within the constraints of the model) as

$$[h'(r) - \omega j(r)] \to \frac{c_0 \delta^2 \mu^2 e^{-r\sqrt{\frac{\mu^2}{1-\delta^4} - \omega^2}}}{r\,(1-\delta^4)\sqrt{\frac{\mu^2}{1-\delta^4} - \omega^2}} + \dots \tag{7.8}$$

From this expression, we immediately see that, keeping only the first terms of the expansions, the oscillatory contributions of h' and ωj cancel each other (even for non-zero δ), so that the difference between h' and ωj corresponds only to the exponential contributions. If we set $\delta = 0$, this difference disappears, and we obtain that the first terms of the asymptotic expansions for h' and ωj are equal to each other, which is consistent with the equation $h' - \omega j = 0$. Therefore, we may expect the following behavior, depending on the value of δ:

- For $\delta \neq 0$ (and within the constraints of the model), h and j decay with exponential and oscillatory contributions, while the spatial part of the magnitude of $\bar{E}$ decays exponentially.
- For $\delta = 0$, h and j decay only with oscillatory contribution. In this case, the solutions for the functions h' and ωj are equal to each other, guaranteeing that the spatial part of the magnitude of $\bar{E}$ is equal to zero.

This behavior is verified directly from the numerical solutions for h and j. Finally, it is crucial to note that this behavior of the system when $\delta = 0$ is valid for our ansatz (5.9)–(5.10), and therefore, it is not a general result for system (5.1). In fact, we can see that if we impose $\delta = 0$ in (5.1) (or in the resulting equations of motion), this results in a complex Maxwell and complex Proca system minimally coupled to gravity. Therefore, in this more general case, setting δ equal to zero does not necessarily imply that the electromagnetic field of the Standard Model disappears.

8 Conclusions

From this proposed model where SFDM possesses a gauge symmetry U(1) whose gauge charge is associated with the dark photon, it is possible to obtain the description of scalar boson stars, both charged and uncharged. Moreover, by considering a spontaneous symmetry breaking in which the dark photon acquires mass, it is possible to obtain Proca-type stars composed of these dark photons.

In the case where the mixing between the dark photon and the SM photon is negligible, the result is the usual mini-Proca stars described in [22], with the only difference being that

JCAP01(2024)018

the mass of the DP is in terms of the effective mass, charge, and self-coupling parameter of the dark matter scalar field. This causes the maximal mass of these Proca stars to be modified in terms of the scalar field parameters.

On the other hand, the presence of the kinetic mixing term between the DP and the SM photon has an influence on the solutions for Proca-type stars. Specifically, the larger the kinetic mixing parameter δ^2, the further the solutions deviate from the pure Proca case. However, when δ^2 takes physical values under the ultralight DP context, the differences in the numerical solutions become increasingly negligible. In this way, we observed that the branches of the ADM mass and the Noether charge as a function of the frequency parameter ω are modified in terms of the kinetic mixing parameter δ^2. In particular, we observed that the usual bound condition for Proca stars is now modified and replaced by (6.6), so the M vs. ω curves possess a shift in the ω axis depending on the value of δ^2. We also found that the maximal ADM mass of each branch varies depending on the value of δ^2; in particular, we found that the larger the δ^2, the smaller the maximal ADM mass of the branch.

Finally, we used the numerical results to calculate the electric field and volumetric energy density associated with the SM electromagnetic field for the case of Proca stars formed by dark photons when the mixing between both photons is not negligible. This is an important result that can help investigate physical observables for these types of stars, in addition to the gravitational effects that are already known.

Additionally, although in the solutions presented in this work we only consider the case where the Proca field associated with the dark photon does not have self-interactions, we include an appendix where we examine the case with self-interactions. We study possible hyperbolicity problems in our model, finding that our model definitely inherits the hyperbolicity issues associated with the self-interacting Proca model, and we address the viability of using methods such as those proposed in [31, 32] to overcome these problems.

Acknowledgments

This work was partially supported by CONACyT México under grants A1-S-8742, 304001, 376127, 240512, FORDECYT-PRONACES grant No. 490769 and I0101/131/07 C-234/07 of the Instituto Avanzado de Cosmología (IAC) collaboration (http://www.iac.edu.mx/).

A Hyperbolicity issues

Motivated by the hyperbolicity issues present in the self-interacting Proca model, in this appendix we study the possible hyperbolicity issues that may be present in our model (2.2). The hyperbolicity issues of Proca model with self-interaction come from the fact that the system can be described by an effective metric that depends on the Proca field itself. The consequence of this is that the hyperbolicity associated with the principal part of the differential operator of Proca's equation may be lost [31, 32]. To study these possible difficulties in our model, we look at the case of the equations for complex electromagnetism and the Proca-type equations that come from the Lagrangian (5.1), which is found after propposing the SSB and approximating to zero the Higgs mode associated with the SFDM. So we start considering a Lagrangian of the form

$$\mathcal{L}_{\rm DP} = -\frac{1}{4}F_{\mu\nu}F^{*\mu\nu} - \frac{1}{4}B_{\mu\nu}B^{*\mu\nu} - U\left(B^2\right) - \frac{\delta^2}{2}R_e\left\{F_{\mu\nu}B^{\mu\nu}\right\}, \tag{A.1}$$

JCAP01(2024)018

where, in the most general case, we consider a potential with quartic self-interaction terms for the Proca field B_μ associated with the dark photon, so

$$U\left(B^2\right) = \frac{1}{2}\mu^2 B_\mu B^{*\mu} + \frac{\mu^2\alpha}{4}\left(B_\mu B^{*\mu}\right)^2 . \tag{A.2}$$

In this case, the equations of motion for A_μ and B_μ are the same as those presented in (5.3) and (5.4), given by

$$\nabla_\mu\left(F^{\mu\nu} + \delta^2 B^{*\mu\nu}\right) = 0, \tag{A.3}$$

$$\nabla_\mu\left(B^{\mu\nu} + \delta^2 F^{*\mu\nu}\right) = 2\hat{U}B^\nu, \tag{A.4}$$

where now $\hat{U} = \frac{dU}{dB^2} = \frac{\mu^2}{2}\left(1 + \alpha B_\mu B^{*\mu}\right)$. We can combine these equations to find a modified Proca equation for B_μ of the form

$$\nabla_\mu B^{\mu\nu} = \frac{2\hat{U}}{(1-\delta^4)}B^\nu. \tag{A.5}$$

From here, we follow the steps presented in [28, 31, 32] to construct the effective metric associated with the principal part of the differential operator in (A.5). We can define $z \equiv \frac{2\hat{U}}{\mu^2}$ and $\varepsilon \equiv (1-\delta^4)$, and consider the case of a real vector field, then $B^2 = B_\mu B^\mu$. So, rewriting (A.5), we have

$$\begin{aligned}
0 &= \nabla_\mu B^{\mu\nu} - \frac{\mu^2 z}{\varepsilon}B^\nu \\
0 &= \nabla^\mu\nabla_\mu B_\nu - \nabla^\mu\nabla_\nu B_\mu - \frac{\mu^2 z}{\varepsilon}B_\nu \\
0 &= \nabla^\mu\nabla_\mu B_\nu - \nabla_\nu\nabla_\mu B^\mu - R_{\mu\nu}B^\mu - \frac{\mu^2 z}{\varepsilon}B_\nu,
\end{aligned} \tag{A.6}$$

where we have used the definitions of the Riemann curvature tensor $\left(\nabla_\mu\nabla_\nu - \nabla_\nu\nabla_\mu\right)B^\mu = R_{\mu\nu}B^\mu$ and $B_{\mu\nu} = \nabla_\mu B_\nu - \nabla_\nu B_\mu$. In addition, from equation (A.5), we have the modified Lorentz condition of the form

$$\nabla_\nu\left(\frac{\mu^2 z}{\varepsilon}B^\nu\right) = 0 \Rightarrow \nabla_\nu B^\nu = -\frac{1}{z}B^\nu\nabla_\nu z, \tag{A.7}$$

putting this in (A.6) we have

$$\begin{aligned}
0 &= \nabla^\mu\nabla_\mu B_\nu - R_{\mu\nu}B^\mu + \frac{1}{z}B^\mu\nabla_\mu\nabla_\nu z - \frac{\mu^2 z}{\varepsilon}B_\nu + \dots \\
0 &= \nabla^\mu\nabla_\mu B_\nu - R_{\mu\nu}B^\mu + \frac{2z'}{z}B^\mu B^\rho\nabla_\mu\nabla_\nu B_\rho - \frac{\mu^2 z}{\varepsilon}B_\nu + \dots \\
0 &= \nabla^\mu\nabla_\mu B_\nu - R_{\mu\nu}B^\mu + \frac{2z'}{z}B_\mu B_\rho\nabla^\mu\nabla^\rho B_\nu + \frac{2z'}{z}B^\mu\nabla_\mu B_{\nu\rho}B^\rho - \frac{\mu^2 z}{\varepsilon}B_\nu + \dots \\
0 &= \nabla^\mu\nabla^\rho B_\nu\left\{z g_{\mu\rho} + 2z' B_\mu B_\rho\right\} + 2z' B^\mu B^\rho\nabla_\mu B_{\nu\rho} - z R_{\mu\nu}B^\mu - \frac{\mu^2 z^2}{\varepsilon}B_\nu + \dots ,
\end{aligned} \tag{A.8}$$

JCAP01(2024)018

where we have followed only the terms with second derivatives and without derivatives. Following exactly the same steps as in [28], in the first line we use $\nabla_\mu \nabla_\nu z = \nabla_\nu \nabla_\mu z$, in the second line we use $\nabla_\nu \left(B_\rho B^\rho\right) = 2B^\rho \nabla_\nu B_\rho$, and in the third line we use the definition of $B_{\mu\nu} = \nabla_\mu B_\nu - \nabla_\nu B_\mu$. Finally, in the last line we multiply by z. In this last equation, by grouping the terms that involve second derivatives, we can introduce the effective metric of the form

$$\hat{g}_{\mu\rho} = z g_{\mu\rho} + 2z' B_\mu B_\rho. \tag{A.9}$$

We can see that, as in the Proca model with self-interactions, our effective metric also depends on B_μ; therefore, we can deduce that the hyperbolicity problems persist in our model (5.1). On the other hand, looking at the terms without derivatives in the last equation, we see that the effective mass matrix in this case is given by

$$M^\mu_\nu = \frac{\mu^2 z^2}{\varepsilon}\delta^\mu_\nu + z R^\mu_\nu, \tag{A.10}$$

which also follows a very similar form to that of the Proca case with self-interactions, except for the term $\varepsilon = (1 - \delta^4)$ that contains the kinetic mixing parameter δ^2. This form of M^μ_ν then also indicates the possible presence of tachyonic instabilities, as mentioned in [28]. One way to try to avoid these problems is to follow the ideas in [31, 32] and try to get a theory of partial UV completion for the Proca model with self-interactions from our model, so that the effective metric in the complete model is the same as the metric of the system and then the hyperbolicity issues disappear (but not necessarily the tachyonic ones). To proceed in this way in our model, it would be necessary to consider the Lagrangian (3.8) obtained from the SSB, and propose that the mass of the Higgs mode is much greater than that of the dark photon. The reason for not proceeding in this way in our model is due to the physical constraints that we consider for the SFDM mentioned in section 3, from these constraints the mass of the Higgs mode would be expected to be much smaller than that of the Proca field associated with the dark photon. Therefore, although the physical constraints for the SFDM in this model may not be compatible with a UV completion theory for the self-interacting Proca model, it is not out of the question to try to apply these ideas to a model like the one proposed in (2.2) within a broader context beyond the one presented in this work.

References

[1] S.U. Ji and S.J. Sin, *Late time phase transition and the galactic halo as a bose liquid. Part 2. The Effect of visible matter*, *Phys. Rev. D* **50** (1994) 3655 [hep-ph/9409267] [INSPIRE].

[2] J.-w. Lee and I.-g. Koh, *Galactic halos as boson stars*, *Phys. Rev. D* **53** (1996) 2236 [hep-ph/9507385] [INSPIRE].

[3] F.S. Guzman and T. Matos, *Scalar fields as dark matter in spiral galaxies*, *Class. Quant. Grav.* **17** (2000) L9 [gr-qc/9810028] [INSPIRE].

[4] J.A. Magaña and T. Matos, *A brief Review of the Scalar Field Dark Matter model*, *J. Phys. Conf. Ser.* **378** (2012) 012012 [arXiv:1201.6107] [INSPIRE].

[5] L.A. Ureña-López, *Brief Review on Scalar Field Dark Matter Models*, *Front. Astron. Space Sci.* **6** (2019) 47 [INSPIRE].

[6] A. Suárez, V.H. Robles and T. Matos, *A Review on the Scalar Field/Bose-Einstein Condensate Dark Matter Model*, in the proceedings of the *4th International Meeting on Gravitation and Cosmology (MGC 4)*, Santa Clara, Villa Clara, Cuba, 1–4 June 2009, *Astrophysics and Space Science Proceedings* **38**, Springer, Cham, Switzerland (2014), pp. 107–142 [DOI:10.1007/978-3-319-02063-1_9] [arXiv:1302.0903] [INSPIRE].

JCAP01(2024)018

[7] T. Rindler-Daller and P.R. Shapiro, *Complex scalar field dark matter on galactic scales*, *Mod. Phys. Lett. A* **29** (2014) 1430002 [arXiv:1312.1734] [INSPIRE].

[8] D.J.E. Marsh, *WarmAndFuzzy: the halo model beyond CDM*, arXiv:1605.05973 [INSPIRE].

[9] J.C. Niemeyer, *Small-scale structure of fuzzy and axion-like dark matter*, *Prog. Part. Nucl. Phys.* **113** (2020) 103787 [arXiv:1912.07064] [INSPIRE].

[10] W. Hu, R. Barkana and A. Gruzinov, *Cold and fuzzy dark matter*, *Phys. Rev. Lett.* **85** (2000) 1158 [astro-ph/0003365] [INSPIRE].

[11] A. Arbey, J. Lesgourgues and P. Salati, *Quintessential haloes around galaxies*, *Phys. Rev. D* **64** (2001) 123528 [astro-ph/0105564] [INSPIRE].

[12] H.L. Bray, *On Dark Matter, Spiral Galaxies, and the Axioms of General Relativity*, arXiv:1004.4016 [INSPIRE].

[13] E.G.M. Ferreira, *Ultra-light dark matter*, *Astron. Astrophys. Rev.* **29** (2021) 7 [arXiv:2005.03254] [INSPIRE].

[14] T. Matos, *The quantum character of the Scalar Field Dark Matter*, *Mon. Not. Roy. Astron. Soc.* **517** (2022) 5247 [arXiv:2211.02025] [INSPIRE].

[15] J. Solís-López, F.S. Guzmán, T. Matos, V.H. Robles and L.A. Ureña-López, *Scalar field dark matter as an alternative explanation for the anisotropic distribution of satellite galaxies*, *Phys. Rev. D* **103** (2021) 083535 [arXiv:1912.09660] [INSPIRE].

[16] C.A.R. Herdeiro, A.M. Pombo, E. Radu, P.V.P. Cunha and N. Sanchis-Gual, *The imitation game: Proca stars that can mimic the Schwarzschild shadow*, *JCAP* **04** (2021) 051 [arXiv:2102.01703] [INSPIRE].

[17] H. Olivares et al., *How to tell an accreting boson star from a black hole*, *Mon. Not. Roy. Astron. Soc.* **497** (2020) 521 [arXiv:1809.08682] [INSPIRE].

[18] I. Sengo, P.V.P. Cunha, C.A.R. Herdeiro and E. Radu, *Kerr black holes with synchronised Proca hair: lensing, shadows and EHT constraints*, *JCAP* **01** (2023) 047 [arXiv:2209.06237] [INSPIRE].

[19] J.C. Bustillo et al., *GW190521 as a Merger of Proca Stars: A Potential New Vector Boson of* 8.7×10^{-13} *eV*, *Phys. Rev. Lett.* **126** (2021) 081101 [arXiv:2009.05376] [INSPIRE].

[20] L. Visinelli, *Boson stars and oscillatons: A review*, *Int. J. Mod. Phys. D* **30** (2021) 2130006 [arXiv:2109.05481] [INSPIRE].

[21] D.J. Kaup, *Klein-Gordon Geon*, *Phys. Rev.* **172** (1968) 1331 [INSPIRE].

[22] R. Brito, V. Cardoso, C.A.R. Herdeiro and E. Radu, *Proca stars: Gravitating Bose-Einstein condensates of massive spin 1 particles*, *Phys. Lett. B* **752** (2016) 291 [arXiv:1508.05395] [INSPIRE].

[23] R. Sharma, S. Karmakar and S. Mukherjee, *Boson star and dark matter*, arXiv:0812.3470 [INSPIRE].

[24] M. Alcubierre, F.S. Guzman, T. Matos, D. Nunez, L.A. Ureña-López and P. Wiederhold, *Galactic collapse of scalar field dark matter*, *Class. Quant. Grav.* **19** (2002) 5017 [gr-qc/0110102] [INSPIRE].

[25] C.A.R. Herdeiro, *Black Holes: On the Universality of the Kerr Hypothesis*, in *Lecture Notes in Physics* **1017**, Springer (2023), pp. 315–331 [DOI:10.1007/978-3-031-31520-6_8] [arXiv:2204.05640] [INSPIRE].

[26] A. Coates and F.M. Ramazanoğlu, *Coordinate Singularities of Self-Interacting Vector Field Theories*, *Phys. Rev. Lett.* **130** (2023) 021401 [arXiv:2211.08027] [INSPIRE].

[27] Z.-G. Mou and H.-Y. Zhang, *Singularity Problem for Interacting Massive Vectors*, *Phys. Rev. Lett.* **129** (2022) 151101 [arXiv:2204.11324] [INSPIRE].

JCAP01(2024)018

[28] A. Coates and F.M. Ramazanoğlu, *Intrinsic Pathology of Self-Interacting Vector Fields*, *Phys. Rev. Lett.* **129** (2022) 151103 [arXiv:2205.07784] [INSPIRE].

[29] E. Barausse, M. Bezares, M. Crisostomi and G. Lara, *The well-posedness of the Cauchy problem for self-interacting vector fields*, *JCAP* **11** (2022) 050 [arXiv:2207.00443] [INSPIRE].

[30] K. Clough, T. Helfer, H. Witek and E. Berti, *Ghost Instabilities in Self-Interacting Vector Fields: The Problem with Proca Fields*, *Phys. Rev. Lett.* **129** (2022) 151102 [arXiv:2204.10868] [INSPIRE].

[31] C. Herdeiro, E. Radu and E. dos Santos Costa Filho, *Proca-Higgs balls and stars in a UV completion for Proca self-interactions*, *JCAP* **05** (2023) 022 [arXiv:2301.04172] [INSPIRE].

[32] K. Aoki and M. Minamitsuji, *Resolving the pathologies of self-interacting Proca fields: A case study of Proca stars*, *Phys. Rev. D* **106** (2022) 084022 [arXiv:2206.14320] [INSPIRE].

[33] T. Matos, A. Perez-Lorenzana and J. Solís-López, *Fermi Bubbles in Scalar Field Dark Matter halos*, arXiv:2203.13218 [INSPIRE].

[34] S. Kumar, U. Kulshreshtha and D. Shankar Kulshreshtha, *Boson stars in a theory of complex scalar fields coupled to the* U(1) *gauge field and gravity*, *Class. Quant. Grav.* **31** (2014) 167001 [arXiv:1605.07210] [INSPIRE].

[35] T. Matos and E. Castellanos, *Phase transition from the symmetry breaking of charged Klein-Gordon fields*, in the proceedings of the *5th Mexican Meeting on Mathematical and Experimental Physics: Recent developments on physics in strong gravitational fields*, Mexico City, Mexico, 9–13 September 2013, *AIP Conf. Proc.* **1577** (2015) 181 [INSPIRE].

[36] T. Matos, E. Castellanos and A. Suárez, *Bose-Einstein condensation and symmetry breaking of a complex charged scalar field*, *Eur. Phys. J. C* **77** (2017) 500 [arXiv:1701.04894] [INSPIRE].

[37] B. Li, T. Rindler-Daller and P.R. Shapiro, *Cosmological Constraints on Bose-Einstein-Condensed Scalar Field Dark Matter*, *Phys. Rev. D* **89** (2014) 083536 [arXiv:1310.6061] [INSPIRE].

[38] C. Herdeiro, I. Perapechka, E. Radu and Y. Shnir, *Asymptotically flat spinning scalar, Dirac and Proca stars*, *Phys. Lett. B* **797** (2019) 134845 [arXiv:1906.05386] [INSPIRE].

[39] F.F. Freitas et al., *Ultralight bosons for strong gravity applications from simple Standard Model extensions*, *JCAP* **12** (2021) 047 [arXiv:2107.09493] [INSPIRE].

[40] A. Caputo, A.J. Millar, C.A.J. O'Hare and E. Vitagliano, *Dark photon limits: A handbook*, *Phys. Rev. D* **104** (2021) 095029 [arXiv:2105.04565] [INSPIRE].

[41] C.A.R. Herdeiro, J.M.S. Oliveira, A.M. Pombo and E. Radu, *Virial identities in relativistic gravity: 1D effective actions and the role of boundary terms*, *Phys. Rev. D* **104** (2021) 104051 [arXiv:2109.05027] [INSPIRE].

[42] J.M.S. Oliveira and A.M. Pombo, *A convenient gauge for virial identities in axial symmetry*, *Phys. Lett. B* **837** (2023) 137646 [arXiv:2207.12451] [INSPIRE].

[43] C.A.R. Herdeiro, J.M.S. Oliveira, A.M. Pombo and E. Radu, *Deconstructing scaling virial identities in general relativity: Spherical symmetry and beyond*, *Phys. Rev. D* **106** (2022) 024054 [arXiv:2206.02813] [INSPIRE].

[44] J.L. Rosa and D. Rubiera-Garcia, *Shadows of boson and Proca stars with thin accretion disks*, *Phys. Rev. D* **106** (2022) 084004 [arXiv:2204.12949] [INSPIRE].

[45] S.L. Liebling and C. Palenzuela, *Dynamical boson stars*, *Living Rev. Rel.* **26** (2023) 1 [arXiv:1202.5809] [INSPIRE].

[46] J.S. Bolton, A. Caputo, H. Liu and M. Viel, *Comparison of Low-Redshift Lyman-α Forest Observations to Hydrodynamical Simulations with Dark Photon Dark Matter*, *Phys. Rev. Lett.* **129** (2022) 211102 [arXiv:2206.13520] [INSPIRE].

JCAP01(2024)018

[47] T. Matos, F.S. Guzman and L.A. Ureña-López, *Scalar field as dark matter in the universe*, *Class. Quant. Grav.* **17** (2000) 1707 [astro-ph/9908152] [INSPIRE].

[48] T. Matos and L.A. Ureña-López, *Quintessence and scalar dark matter in the universe*, *Class. Quant. Grav.* **17** (2000) L75 [astro-ph/0004332] [INSPIRE].

[49] V. Sahni and L.-M. Wang, *A New cosmological model of quintessence and dark matter*, *Phys. Rev. D* **62** (2000) 103517 [astro-ph/9910097] [INSPIRE].

[50] T. Matos, A. Suárez and J.A. Magaña, *Structure formation with scalar field dark matter*, in the proceedings of the *8th Mexican School on Gravitation and Mathematical Physics: Speakable and unspeakable in gravitational physics*, Playa del Carmen, Quintana Roo, Mexico, 6–12 December 2009, *AIP Conf. Proc.* **1256** (2010) 283 [INSPIRE].

[51] M.S. Turner, *Coherent Scalar Field Oscillations in an Expanding Universe*, *Phys. Rev. D* **28** (1983) 1243 [INSPIRE].

[52] F. Briscese, *Viability of complex self-interacting scalar field as dark matter*, *Phys. Lett. B* **696** (2011) 315 [arXiv:1101.0028] [INSPIRE].

[53] M. Su, T.R. Slatyer and D.P. Finkbeiner, *Giant Gamma-ray Bubbles from Fermi-LAT: AGN Activity or Bipolar Galactic Wind?*, *Astrophys. J.* **724** (2010) 1044 [arXiv:1005.5480] [INSPIRE].

[54] FERMI-LAT collaboration, *The Spectrum and Morphology of the Fermi Bubbles*, *Astrophys. J.* **793** (2014) 64 [arXiv:1407.7905] [INSPIRE].

[55] A. Arbey and F. Mahmoudi, *Dark matter and the early Universe: a review*, *Prog. Part. Nucl. Phys.* **119** (2021) 103865 [arXiv:2104.11488] [INSPIRE].

[56] K. Freese, *Review of Observational Evidence for Dark Matter in the Universe and in upcoming searches for Dark Stars*, *EAS Publ. Ser.* **36** (2009) 113 [arXiv:0812.4005] [INSPIRE].

[57] M.Y. Khlopov, *Introduction*, *Mod. Phys. Lett. A* **32** (2017) 1702001 [arXiv:1704.06511] [INSPIRE].

[58] L.H. Ryder, *Quantum Field Theory*, second edition, Cambridge University Press (1996) [DOI:10.1017/CBO9780511813900] [INSPIRE].

[59] W.S. Gan, *Gauge Invariance Approach to Acoustic Fields*, Springer, Singapore (2019) [DOI:10.1007/978-981-13-8751-7].

[60] T. Lancaster and S. Blundell, *Quantum field theory for the gifted amateur*, Oxford University Press, Oxford, U.K. (2014).

[61] F.E. Schunck and E.W. Mielke, *General relativistic boson stars*, *Class. Quant. Grav.* **20** (2003) R301 [arXiv:0801.0307] [INSPIRE].

[62] R. Ruffini and S. Bonazzola, *Systems of selfgravitating particles in general relativity and the concept of an equation of state*, *Phys. Rev.* **187** (1969) 1767 [INSPIRE].

[63] D. Antypas et al., *New Horizons: Scalar and Vector Ultralight Dark Matter*, in the proceedings of the *Snowmass 2021*, Seattle, WA, U.S.A., 17–26 July 2022, arXiv:2203.14915 [INSPIRE].

[64] Z. Meliani, F.H. Vincent, P. Grandclément, E. Gourgoulhon, R. Monceau-Baroux and O. Straub, *Circular geodesics and thick tori around rotating boson stars*, *Class. Quant. Grav.* **32** (2015) 235022 [arXiv:1510.04191] [INSPIRE].

[65] P. Grandclement, C. Somé and E. Gourgoulhon, *Models of rotating boson stars and geodesics around them: new type of orbits*, *Phys. Rev. D* **90** (2014) 024068 [arXiv:1405.4837] [INSPIRE].

[66] F.H. Vincent, Z. Meliani, P. Grandclement, E. Gourgoulhon and O. Straub, *Imaging a boson star at the Galactic center*, *Class. Quant. Grav.* **33** (2016) 105015 [arXiv:1510.04170] [INSPIRE].

JCAP01(2024)018

[67] P.V.P. Cunha, C.A.R. Herdeiro, E. Radu and H.F. Runarsson, *Shadows of Kerr black holes with and without scalar hair*, *Int. J. Mod. Phys. D* **25** (2016) 1641021 [arXiv:1605.08293] [INSPIRE].

[68] H. Dehnen and B. Rose, *Flat rotation curves of spiral galaxies and the dark matter particles*, *Astrophys. Space Sci.* **207** (1993) 133.

[69] F. García and I.S. Landea, *Charged Proca Stars*, *Phys. Rev. D* **94** (2016) 104006 [arXiv:1608.00011] [INSPIRE].

[70] M. Minamitsuji, *Vector boson star solutions with a quartic order self-interaction*, *Phys. Rev. D* **97** (2018) 104023 [arXiv:1805.09867] [INSPIRE].

[71] R. Brito, V. Cardoso, C.F.B. Macedo, H. Okawa and C. Palenzuela, *Interaction between bosonic dark matter and stars*, *Phys. Rev. D* **93** (2016) 044045 [arXiv:1512.00466] [INSPIRE].

[72] J. Jaeckel, *A force beyond the Standard Model-Status of the quest for hidden photons*, in *Frascati Physics Series* **56**, INFN Publications (2012), pp. 172–192 [arXiv:1303.1821] [INSPIRE].

[73] T. Sato, F. Takahashi and M. Yamada, *Gravitational production of dark photon dark matter with mass generated by the Higgs mechanism*, *JCAP* **08** (2022) 022 [arXiv:2204.11896] [INSPIRE].

[74] G. Alonso-Álvarez, F. Ertas, J. Jaeckel, F. Kahlhoefer and L.J. Thormaehlen, *Hidden Photon Dark Matter in the Light of XENON1T and Stellar Cooling*, *JCAP* **11** (2020) 029 [arXiv:2006.11243] [INSPIRE].

[75] P. Agrawal, N. Kitajima, M. Reece, T. Sekiguchi and F. Takahashi, *Relic Abundance of Dark Photon Dark Matter*, *Phys. Lett. B* **801** (2020) 135136 [arXiv:1810.07188] [INSPIRE].

[76] P. Adshead and K.D. Lozanov, *Self-gravitating Vector Dark Matter*, *Phys. Rev. D* **103** (2021) 103501 [arXiv:2101.07265] [INSPIRE].

[77] M.A. Amin, M. Jain, R. Karur and P. Mocz, *Small-scale structure in vector dark matter*, *JCAP* **08** (2022) 014 [arXiv:2203.11935] [INSPIRE].

[78] A. Denig, *Review of dark photon searches*, *EPJ Web Conf.* **130** (2016) 01005 [INSPIRE].

[79] F. Curciarello, *Review on Dark Photon*, *EPJ Web Conf.* **118** (2016) 01008 [INSPIRE].

[80] G.N. Wojcik and T.G. Rizzo, *Forbidden scalar dark matter and dark Higgses*, *JHEP* **04** (2022) 033 [arXiv:2109.07369] [INSPIRE].

[81] L. Su, L. Wu and B. Zhu, *Probing for an ultralight dark photon from inverse Compton-like scattering*, *Phys. Rev. D* **105** (2022) 055021 [arXiv:2105.06326] [INSPIRE].

[82] M. Redi and A. Tesi, *Dark photon Dark Matter without Stueckelberg mass*, *JHEP* **10** (2022) 167 [arXiv:2204.14274] [INSPIRE].

[83] C. Mondino, M. Pospelov, J.T. Ruderman and O. Slone, *Dark Higgs Dark Matter*, *Phys. Rev. D* **103** (2021) 035027 [arXiv:2005.02397] [INSPIRE].

[84] M. Gorghetto, E. Hardy, J. March-Russell, N. Song and S.M. West, *Dark photon stars: formation and role as dark matter substructure*, *JCAP* **08** (2022) 018 [arXiv:2203.10100] [INSPIRE].

[85] G. Marocco, *Dark photon limits from magnetic fields and astrophysical plasmas*, arXiv:2110.02875 [INSPIRE].

[86] M. Fabbrichesi, E. Gabrielli and G. Lanfranchi, *The Dark Photon*, in *SpringerBriefs in Physics*, Springer, Cham, Switzerland (2021) [arXiv:2005.01515] [DOI:10.1007/978-3-030-62519-1] [INSPIRE].

[87] M. Fabbrichesi, E. Gabrielli and G. Lanfranchi, *The Dark Photon*, in *SpringerBriefs in Physics*, Springer, Cham, Switzerland (2021) [arXiv:2005.01515] [DOI:10.1007/978-3-030-62519-1] [INSPIRE].

JCAP01(2024)018

[88] S.M. Carroll, *Spacetime and Geometry: An Introduction to General Relativity*, first edition, Cambridge University Press (2019) [DOI:10.1017/9781108770385] [INSPIRE].

[89] E.E. Jenkins, A.V. Manohar and M. Trott, *On Gauge Invariance and Minimal Coupling*, *JHEP* **09** (2013) 063 [arXiv:1305.0017] [INSPIRE].

[90] V.C. Rubin and W.K. Ford Jr., *Rotation of the Andromeda Nebula from a Spectroscopic Survey of Emission Regions*, *Astrophys. J.* **159** (1970) 379 [INSPIRE].

[91] I.M. Anderson, *The principle of minimal gravitational coupling*, *Arch. Ration. Mech. Anal.* **75** (1981) 349.

[92] I. Melo, *Higgs potential and fundamental physics*, *Eur. J. Phys.* **38** (2017) 065404 [arXiv:1911.08893] [INSPIRE].

[93] G. Bertone and M.P.T. Tait, *A new era in the search for dark matter*, *Nature* **562** (2018) 51 [arXiv:1810.01668] [INSPIRE].

[94] L. Bergström, *Dark Matter Evidence, Particle Physics Candidates and Detection Methods*, *Ann. Phys.* **524** (2012) 479 [arXiv:1205.4882] [INSPIRE].

[95] C.L. Lewis, *Explicit gauge covariant Euler-Lagrange equation*, *Am. J. Phys.* **77** (2009) 839 [arXiv:0907.2301] [INSPIRE].

[96] U. Keshet and I. Gurwich, *Fermi bubbles: high latitude X-ray supersonic shell*, *Mon. Not. Roy. Astron. Soc.* **480** (2018) 223 [arXiv:1704.05070] [INSPIRE].

[97] N. Sanchis-Gual, C. Herdeiro, E. Radu, J.C. Degollado and J.A. Font, *Numerical evolutions of spherical Proca stars*, *Phys. Rev. D* **95** (2017) 104028 [arXiv:1702.04532] [INSPIRE].

[98] A.M. Pombo, J.M.S. Oliveira and N.M. Santos, *Coupled scalar-Proca soliton stars*, *Phys. Rev. D* **108** (2023) 044044 [arXiv:2304.13749] [INSPIRE].

JCAP01(2024)018